

Theoretical interpretation of multiphoton ionization of neon by soft-x-ray intense radiation

M. G. Makris¹ and P. Lambropoulos^{1,2}

¹*Institute of Electronic Structure and Laser, Foundation of Research and Technology Hellas,
P. O. Box 1527, Herakleion 71110, Crete, Greece*

²*Department of Physics, University of Crete, P. O. Box 2208, Herakleion 71003, Crete, Greece*

(Received 13 June 2007; published 1 February 2008)

We present an attempt at the theoretical interpretation of recent experimental results on multiphoton ionization of neon by photons of energies 38.4 and 42.8 eV at the free electron laser facility [A. A. Sorokin *et al.*, Phys. Rev. A **75**, 051402(R) (2007)]. Although, given the photon energies, the intensities employed place the process within the regime of perturbation theory, effects such as the pulsed nature of the field and expansion of the interaction volume need to be and are taken into consideration. The values of some of the cross sections are obtained through scaling and given the semiquantitative nature of the calculations, overall reasonable agreement with the experimental data is found, although some issues pertaining to details remain as questions.

DOI: [10.1103/PhysRevA.77.023401](https://doi.org/10.1103/PhysRevA.77.023401)

PACS number(s): 32.80.Rm, 32.80.Fb, 42.50.Hz

I. INTRODUCTION

The first experiments on multiphoton ionization under the new free electron laser (FEL) xuv sources have produced results with photons in the energy range between about 10 and 100 eV [1–3]. The intensities have so far been below 10^{16} W/cm² which places the process of ionization well within the regime of lowest order perturbation theory (LOPT). Since multiple ionization has been observed in the rare gases, it is expected to be sequential, an established term implying the sequential stripping of electrons from successive ionic species. Depending on the photon energy, this stripping may begin with electrons from the valence or subvalence shells.

In multiphoton multiple ionization experiments under infrared and optical lasers over the last 30 years or so (Ref. [4], and references therein), the stripping has involved only valence electrons, no matter how large the laser intensity was. Even under conditions, namely, sufficiently intense pulses of short (subpicosecond) duration, where nonsequential double ionization has been observed, it is valence electrons that were ejected. This is due to the long wavelength (~ 780 – 800 nm) of the radiation employed in those experiments. It is well known that subvalence electrons are screened by the outer ones, especially in closed-shell atoms such as the rare gases. As a result, radiation of infrared and optical wavelengths cannot “penetrate” below the valence shell, and that is why even extremely strong infrared radiation, possessing more than sufficient energy to eject electrons from inner subshells, never does. It is only after the outer shell has been opened by the ejection of one or more electrons that it may become possible to excite an electron from the shell just below, namely, ns^2 in a rare gas with outer shell np^6 . A case in point can be found in Ref. [5].

This situation is expected to be entirely different when the wavelength becomes sufficiently short to reach subvalence shells directly. For example, in the atom of xenon, with an ionization potential of about 12 eV, under radiation of photon energy around 90–100 eV, the stripping would be expected to begin with electrons predominantly from the $4d$ shell. This process should continue more or less until an ionic species of

$4d$ ionization threshold more than 100 eV is reached, which for the case of xenon would be Xe^{3+} . From there on, the stripping will continue with electrons removed from the outer shell of the successive ions. In fact, a preliminary analysis of recent experiments [6] along those lines appears to provide the first indication of such a process of stripping from the inside. Needless to say, as photons of even higher energy become available, the stripping will begin with electrons from even lower shells. A very important point to be kept in mind is the following: If perturbation theory is valid for the ejection of the first electron, it will be even more so for all subsequent species as they are increasingly more strongly bound (higher ionization potentials).

Whether the stripping begins from the inside or the outside, as is the case in the problem and conditions under consideration in this paper, the process can be described in terms of differential equations governing the evolution of ionic species during the laser pulse. Two pieces of theoretical information are needed in this description: (a) The relevant single-photon or multiphoton ionization cross sections, and (b) a reasonably realistic model for the temporal evolution of the pulse; including, if deemed necessary, its spatial distribution in the interaction region.

This type of approach has a long history and has been found useful in a variety of contexts [4,5,7]. In the infrared and optical spectral range, the relevant cross sections, mostly of relatively low order (say up to 5), had over the years been calculated for a variety of atomic and in some cases molecular species. With the exception of atomic hydrogen, however, it is rather impractical to attempt the calculation of higher order cross sections. Fortunately, that is not really necessary, especially in so far as semiquantitative theory is concerned. As shown in Ref. [4], some time ago, higher order multiphoton cross sections exhibit, in general, a rather smooth dependence on photon energy. Moreover, due to the relatively broad bandwidth of short pulses, such as those found in the short wavelength FEL sources, even if the central frequency happens to be in resonance with some intermediate state, the effective cross section is smoothed out. As a result, one can employ a procedure of scaling which takes into consideration the ionization potential and the size of the species. The details of this procedure, as well as some early applications,

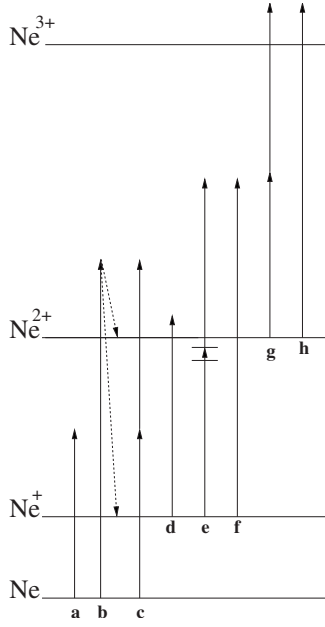


FIG. 1. Pathways for (multiple) ionization of Ne in the photon energy range under consideration up to Ne^{3+} : (a) Single-photon ionization of Ne, (b) single-photon single and double ionization of Ne (harmonic), (c) two-photon double ionization of Ne, (d) single-photon single ionization of Ne^+ , (e) two-photon single ionization of Ne^+ , (f) single-photon single ionization of Ne^+ (harmonic), (g) two-photon single ionization of Ne^{2+} , and (h) single-photon single ionization of Ne^{2+} (harmonic).

can be found in Ref. [4]. Eventually, as experimental data are refined, some realistic calculations of multiphoton cross sections must be made. At this early stage of the field, however, it is worthwhile to explore some basic features of these processes using the scaling approach, which is the purpose of this paper. We have chosen the photon energies 38.4 eV and 42.8 eV, for which some first experimental results are already available [1].

II. THEORETICAL FORMULATION

Although, in principle, the initial neutral atom can be stripped of all of its electrons, in reality only a certain number of ionic species will be produced in a quantity significant enough to be included in the calculation. This of course depends on the intensity and pulse duration and the decision on how many should be included must be made in the process of the calculation. For the range of intensity and duration under consideration in this paper it suffices to include species up to Ne^{4+} . On the same grounds, we include in our framework low-order processes, first and second order with the fundamental of the FEL (unless the ionization requires explicitly higher order) and only first order for the harmonic of the FEL due to its substantially lower intensity. Processes under consideration leading to the production of up to Ne^{3+} are shown in Fig. 1; subsequent ionization of Ne^{3+} is possible only by three-photon absorption of the FEL fundamental in the energy range (~ 40 eV) under consideration. One

could raise the question as to whether ionization pathways involving excited ions (Ne^{+*} and Ne^{2+*}) should also be considered. A careful analysis, however, reveals that these channels are of no importance. Thus, we are led to the following set of rate equations for the different species of Ne:

$$\dot{N}_0 = -\sigma_{01}^{(1)}F(t)N_0 - \sigma_{02}^{(2)}F^2(t)N_0 - \sigma_{01}^{(1)}F^h(t)N_0 - \sigma_{02}^{(1)}F^h(t)N_0,$$

$$\begin{aligned} \dot{N}_1 &= \sigma_{01}^{(1)}F(t)N_0 - \sigma_{12}^{(1)}F(t)N_1 - \sigma_{12}^{(2)}F^2(t)N_1 + \sigma_{01}^{(1)}F^h(t)N_0 \\ &\quad - \sigma_{12}^{(1)}F^h(t)N_1, \end{aligned}$$

$$\begin{aligned} \dot{N}_2 &= \sigma_{02}^{(2)}F^2(t)N_0 + \sigma_{12}^{(1)}F(t)N_1 + \sigma_{12}^{(2)}F^2(t)N_1 - \sigma_{23}^{(2)}F^2(t)N_2 \\ &\quad + \sigma_{12}^{(1)}F^h(t)N_1 + \sigma_{02}^{(1)}F^h(t)N_0 - \sigma_{23}^{(1)}F^h(t)N_2, \end{aligned}$$

$$\dot{N}_3 = \sigma_{23}^{(2)}F^2(t)N_2 - \sigma_{34}^{(3)}F^3(t)N_3 + \sigma_{23}^{(1)}F^h(t)N_2,$$

$$\dot{N}_4 = \sigma_{34}^{(3)}F^3(t)N_3,$$

where N_0 and $N_{i=1,2,3,4}$ represent the population of neutral Ne and the first four ionized species, $F(t)$ and $F^h(t)$ represent the photon flux of the FEL pulse and its second harmonic, respectively, and σ represents the cross sections for the respective processes. The superscript in the cross sections denotes the order of the process and the subscript stands for the initial and final species. The term $\sigma_{12}^{(1)}F(t)N_1$ that couples N_1 and N_2 with one photon transition is absent for photon energy 38.4 eV, i.e., below the ionization threshold of 40.96 eV of Ne^+ . This is essentially the only difference in the physical description of the ionization process between the above two photon energies under consideration.

Concerning now the FEL pulse, we opt to leave aside for the moment small scale temporal structure of intensity, by considering a Gaussian pulse of full width at half-maximum of 25 fs. The ever present second harmonic of the FEL beam is also taken into account assuming the same time dependence as the fundamental. A space average of the species production is essential for the intensity range under consideration and is thus included by employing a space profile of the intensity at the focus of the FEL resembling the one in Ref. [8], with a weak intensity dependence along the propagation axes in the detector window of ≈ 1 mm).

The cross sections needed in this case are, to our knowledge, only partly known; in the photon energy range of interest here, $\sigma_{01}^{(1)} \approx 8$ Mb at 40 eV, $\sigma_{01}^{(1)} \approx 5$ Mb at 80 eV (e.g., see Refs. [9,10]), $\sigma_{02}^{(1)} \approx 0.2$ Mb [11,12], and $\sigma_{12}^{(1)} \approx 5$ Mb [13]. The rest of the cross sections are estimated by scaling these cross sections or the respective cross sections of He for similar processes, in the spirit of Ref. [4]. We must note, however, that due to the low order of the cross sections we intend to obtain by scaling, some modifications on the approach of Ref. [4] are in order. In particular, we can no longer assume an average value for the energy denominator in the expression for the cross section [Eq. (8) of Ref. [4]] which is a good approximation only for high-order processes. In fact, this issue does not arise for single-photon processes. For the two- and three-photon processes we must scale, it so happens that there are no nearby resonances for both He and Ne, with

TABLE I. Experimental cross sections available for Ne and their corresponding theoretical estimates. The values depicted in the third column (Estimate I) have been obtained by scaling Ne cross sections, whereas the values of the fourth column (Estimate II) are theoretical estimates based on the cross sections for He presented in the last column. For the first six rows the photon energy is ≈ 40 eV and for the last four rows ≈ 80 eV, respectively. Respective processes: (a) $\text{He} + \hbar\omega \rightarrow \text{He}^+$ (Refs. [18–20]), (b) $\text{He} + 2\hbar\omega \rightarrow \text{He}^+$ (Ref. [15]), (c) $\text{He} + 2\hbar\omega \rightarrow \text{He}^{2+}$ (Ref. [16]), (d) $\text{He} + 3\hbar\omega \rightarrow \text{He}^+$ (Ref. [14]), (e) $\text{He} + \hbar\omega \rightarrow \text{He}^{2+}$ (Ref. [12]), (f) $\text{Ne} + \hbar\omega \rightarrow \text{Ne}^+$ (Refs. [9,10,12]), (g) $\text{Ne}^+ + \hbar\omega \rightarrow \text{Ne}^{2+}$ (Ref. [13]).

Cross section	Expt.	Ne		He
		Estimate I	Estimate II	Expt./theory
$\sigma_{01}^{(1)}(\text{cm}^2)$	8×10^{-18} (f) ^a			2.5×10^{-18} (a)
$\sigma_{12}^{(1)}(\text{cm}^2)$	5×10^{-18} (g) ^a	6×10^{-18} (f)	2.2×10^{-17}	6.8×10^{-18} (a)
$\sigma_{02}^{(2)}(\text{cm}^4 \text{ s})$			8×10^{-51} a	8×10^{-52} (c)
$\sigma_{12}^{(2)}(\text{cm}^4 \text{ s})$			2×10^{-51} a	8×10^{-52} (c)
$\sigma_{23}^{(2)}(\text{cm}^4 \text{ s})$			1×10^{-50} a	1×10^{-51} (b)
$\sigma_{34}^{(3)}(\text{cm}^6 \text{ s}^2)$			1.5×10^{-83} a	5×10^{-85} (d)
$\sigma_{01}^{(1)}(\text{cm}^2)$	5×10^{-18} (f) ^a			
$\sigma_{02}^{(1)}(\text{cm}^2)$	0.2×10^{-18} (f) ^a		0.1×10^{-18}	1×10^{-20} (e)
$\sigma_{12}^{(1)}(\text{cm}^2)$	5×10^{-18} (g) ^{a,b}	8×10^{-18} (f)	6.4×10^{-18}	2×10^{-18} (a)
$\sigma_{23}^{(1)}(\text{cm}^2)$		8×10^{-18} (f)/ 7×10^{-18} (g) ^a	16×10^{-18}	5×10^{-18} (a)

^aThe cross sections employed in the calculations.

^bExtrapolated.

the exceptions of two-photon single ionization of Ne^+ and three-photon single ionization of He which we address later on. This allows us to neglect the scaling of the cross section due to the different ionization potentials of the Ne and He species. Moreover, the radii of the first few species of Ne do not change appreciably ($\approx 25\%$ from Ne to Ne^{4+}), so the change of the cross section due to the variation of the size of the atom can safely be neglected. We thus arrive at a simplified version of the scaling procedure, where in the case we employ Ne cross sections, we scale only the photon energy and in the case we employ He cross sections we also take into account the different size of the two atoms through the ratio of $\sigma_{01}^{\text{Ne}}/\sigma_{01}^{\text{He}}$ as obtained from experimental data. Due to the relative proximity of the photon energies under consideration, the cross sections we end up with are essentially the same.

Let us look at an example of how scaling is applied in calculating $\sigma_{02}^{(1)}$ for a harmonic photon energy of 80 eV, as an indication of the approximation level we expect. $\sigma_{02}^{(1)}$ should be scaled to the double ionization potential of He leading to a corresponding photon energy of $80 \frac{79}{62.5} \approx 100$ eV, for which the single-photon double ionization of He is $\sigma_{02}^{(1)} \approx 10$ Kb (Ref. [12]). To convert it to a Ne cross section, it should be multiplied by $(\sigma_{01}^{\text{Ne}}/\sigma_{01}^{\text{He}})^2$ since this is a transition involving two electrons. The cross section we arrive at is 0.1 Mb which compares well with the experimental value of 0.2 Mb, since a factor of 2 is more than adequate for our purposes. Following the same approach, $\sigma_{12}^{(1)}$ and $\sigma_{23}^{(1)}$ are scaled to the single-photon single ionization of He and Ne, and $\sigma_{12}^{(2)}$, $\sigma_{23}^{(2)}$ are scaled to the two-photon double ionization of He, with results shown in Table I.

A note is worthwhile for $\sigma_{34}^{(3)}$ since the scaled photon energies for three-photon single ionization of He are about 9.7

and 10.8 eV, falling around a resonance as depicted in Fig. 2 of Ref. [14]. Since there is no nearby resonance in the Ne^{3+} three-photon ionization, we must use the background cross section of He in this energy region leaving aside the contribution of the nearby resonances. We thus estimate the smooth background cross section to be around $5 \times 10^{-85} \text{ cm}^6 \text{ s}^2$ leading to a cross section of Ne of $1.5 \times 10^{-83} \text{ cm}^6 \text{ s}^2$.

Also we must be careful in the scaling procedure for $\sigma_{12}^{(2)}$ which is somewhat more complicated. First, there are bound states of the He atom in the energy range of the scaled photon energies, i.e., 23.0 and 25.7 eV. We can nevertheless estimate the smooth background of the cross section to be around $2 \times 10^{-52} \text{ cm}^4 \text{ s}$ (see Fig. 4 of Ref. [15]). There are some intermediate bound states in the two-photon single ionization of Ne^+ for the 38.4 eV photon, with the closest one ($2s^2 2p^4 4s$ at 38.2 eV) falling well inside the reported Ref. [1] bandwidth (0.4 eV) of the laser pulse, the laser bandwidth which is of the same order as the detuning. The width of the nearby states, however, are expected to be much smaller than that, as a result of which, one would not expect a significant enhancement due to the nearby states. A possible exception to this expectation might result from either a strong Rabi oscillation between the initial and intermediate states, or from large ionization width (of the order of the laser bandwidth) of the intermediate state. In a different language, this would occur if either the bound-bound or bound-free transition is saturated. In that event, the intensity dependence of the Ne^{2+} signal should deviate perceptively from the expected I^2 dependence, for which there is no hint in the rather limited intensity range of the experimental data. In addition, as is evident in Fig. 2, such a deviation would be masked by the volume expansion effect which sets in below 10^{13} W/cm^2 . Nevertheless, this is an issue that may require

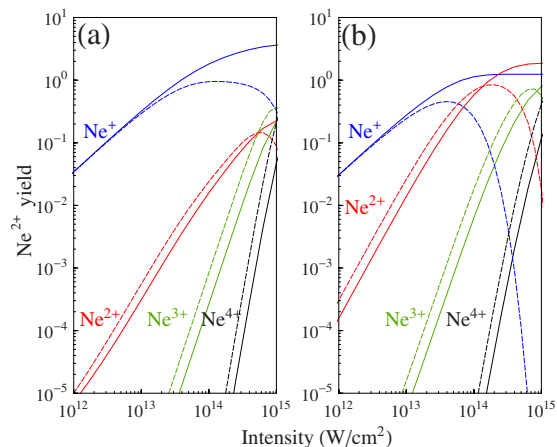


FIG. 2. (Color online) Ionization yield of Ne species with (solid lines) and without (dashed lines) space average, for Ne^+ , Ne^{2+} , Ne^{3+} , and Ne^{4+} (blue, red, green, and black, respectively). In (a) and (b) photon energy is just below and above the single-photon ionization threshold of Ne^+ (38.4 and 42.8 eV, respectively). Space average is normalized on the Ne^+ production at low intensities and the intensity of the second harmonic of the FEL has been taken as 10^{-2} of the fundamental.

closer inspection when more extensive data become available.

III. RESULTS

In Fig. 2 we present the predicted ion signals of Ne, for the photon energies under consideration, above and below the Ne^+ single-photon ionization threshold and for intensities in the range of 10^{12} to 10^{15} W/cm^2 . Including the space average in the calculation proves to be essential even for intensities lower than 10^{13} W/cm^2 . The different intensity dependence of the species production is both evident and expected, with the abundance of all species being influenced in this intensity range by the bottleneck of two-photon ionization of Ne^+ for photon energy below the threshold of single-photon ionization. This bottleneck effectively leads to a time window inside the pulse where Ne^{2+} is mainly produced. Approximately the same time window is open for Ne^{3+} and a shorter one for Ne^{4+} , since it is accessible only via a three-photon process. This effectively leads to a congestion of species production at higher intensities, and alters their respective abundances. Even for intensities as high as 10^{15} W/cm^2 the most abundant species is Ne^+ (space averaged) in this case, whereas for photon energy above the Ne^+ ionization threshold the most abundant species are Ne^{2+} and Ne^{3+} .

The relative importance of each separate pathway in the production or depletion of the various Ne species can be tracked down by solving, in parallel with the set of the differential equations for the populations, the differential equation for each pathway separately. For instance, the contribution of pathway (b) of Fig. 1 in Ne^{2+} production is derived from the solution of $\dot{N}_{2,b} = \sigma_{02}^{(2)} F^2(t) N_0$. In general, the exact intensity range where different processes dominate in the

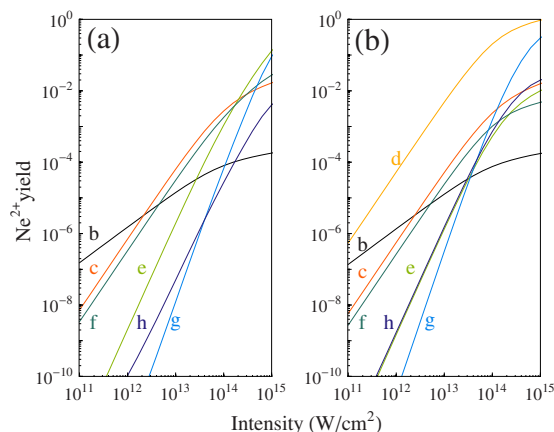


FIG. 3. (Color online) Space averaged Ne^{2+} population produced or annihilated by the different channels depicted in Fig. 1. The intensity of the harmonic is 10^{-2} of the FEL intensity and the photon energy in the left- and right-hand graphs is 38.4 eV and 42.8 eV, respectively.

production or depletion of each species depends on the values of the cross sections and the relative intensity of the harmonic of the FEL. Nevertheless, the important features are present and as an example we consider the Ne^{2+} since it is sensitive to the difference of the photon energies under consideration. In Fig. 3, the contributions of all different channels in the production and depletion of Ne^{2+} are depicted, showing a clear qualitative difference. Above the threshold for one-photon ionization of Ne^+ , Ne^{2+} is predominantly produced throughout the intensity range of 10^{11} to 10^{15} W/cm^2 by single-photon single ionization of Ne^+ , with the rest of the pathways having a contribution more than one order of magnitude smaller. On the other hand, below the threshold the dominant pathways are intensity dependent. For low intensities, single-photon double ionization of Ne by the harmonic of the FEL dominates and as the intensity increases it is eventually taken over at about 10^{12} W/cm^2 by two-photon double ionization of neutral Ne and single-photon ionization of Ne^+ by the harmonic. For intensities higher than 10^{14} W/cm^2 , Ne^{2+} is predominantly produced via two-photon double ionization of Ne^+ by the fundamental. The dominant pathway, however, is very sensitive to the values of the cross sections employed. A factor of 2 or 3 can make a difference as to which channel dominates and the exact intensity range it does so, especially for processes of the same order. This would not be a quantitative change only, but a qualitative one and here we offer insight on the relative weight of different pathways. A further refinement would require the quantitative calculation of the few photon cross sections involved, which would be more meaningful when more extensive experimental data become available.

The ratios of the different Ne species are shown in Fig. 4 with the second harmonic of the FEL intensity varied up to 10^{-2} of the fundamental. In Fig. 4(a) the unknown cross sections are obtained by scaling, and do not reproduce the slope reported in the experiment. This happens because in the intensity range of the experiment, Ne^{2+} is produced via two-photon double ionization of neutral Ne and single-photon

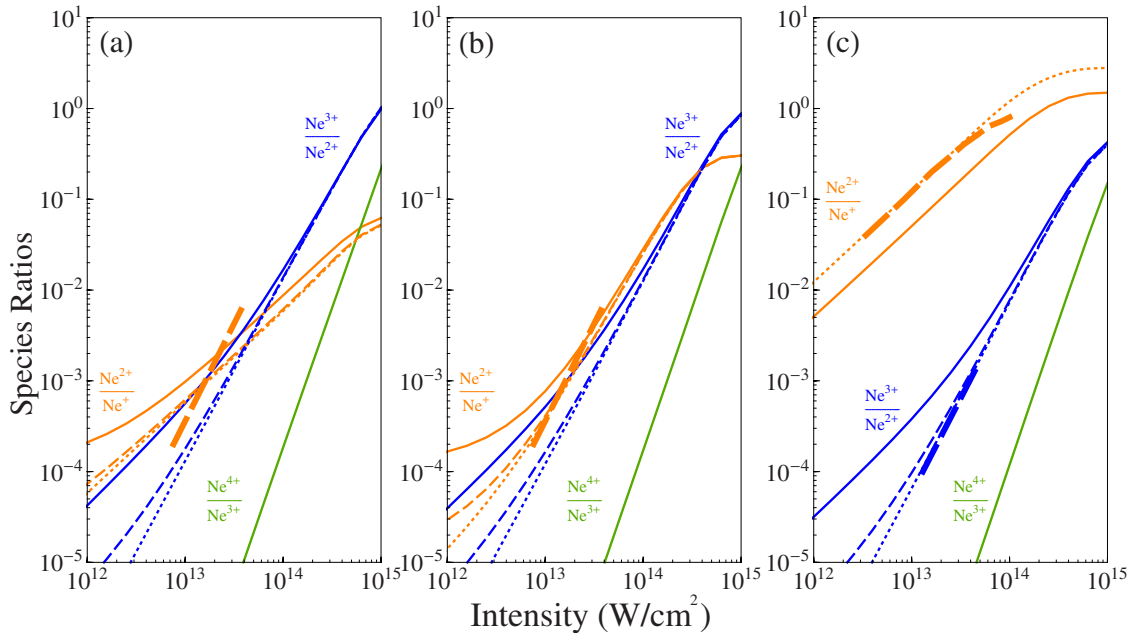


FIG. 4. (Color online) Space averaged ratios of Ne species employing the scaled cross sections [(a) and (c)] and cross sections to fit the experimental data (b). $\text{Ne}^{2+}/\text{Ne}^+$, $\text{Ne}^{3+}/\text{Ne}^{2+}$, $\text{Ne}^{4+}/\text{Ne}^{3+}$ depicted in orange, blue, and green, respectively. The intensity of the harmonic is 10^{-2} , 10^{-3} , and 0 of the FEL intensity for the solid, dashed, and dotted curves, respectively. The cases where harmonic intensity does not influence the species ratio is not shown so as to avoid congesting the figure. For panel (c) only, the orange dotted curve is obtained with $\sigma_{12}^{(1)} = 12$ Mb. Heavy dashed lines represent the respective experimental data of Ref. [1]. In (a) and (b) the photon energy is 38.4 eV and in (c) 42.8 eV, respectively.

ionization of Ne^+ with the harmonic, so the ratio $\text{Ne}^{2+}/\text{Ne}^+$ appears in our calculations with a slope of 1. For a slope comparable to 2 to appear, we must lower the $\sigma_{02}^{(2)}$ to a fifth of the value suggested in Table I and keep the intensity of the harmonic below 10^{-3} of the FEL intensity. Since the ratio is then displaced downwards upon these modifications of the cross sections, we also must consider a σ_{12}^2 15 times higher than predicted, so as to finally arrive at a ratio with slope and magnitude [Fig. 4(b)] compatible with the data of Ref. [1]. This is a rather large value for a two-photon cross section for an atom such as neon. Whether the presence of a nearby resonance could have played a role is rather debatable, in view of the substantial bandwidth of the FEL.

For the 42.8 eV photon, the ratio $\text{Ne}^{2+}/\text{Ne}^+$ above threshold is insensitive to the presence of the harmonic, since both species are predominantly produced by single-photon processes with the FEL fundamental, i.e., channels (a) and (d) of Fig. 1. The ratio we arrive at is smaller by a factor of about 2 compared to the experiment of [1], with the latter fitted with a value of $\sigma_{12}^{(1)} = 12$ Mb, with $\sigma_{01}^{(1)} = 8$ Mb [Fig. 4(b), red dotted curve]. We must note here that the important cross sections employed in our calculations are known from previous experiments [9,10,13], so a factor of about 2 is an important difference, since as far as these two species are concerned our calculations can be considered quantitative and not qualitative. Finally, the change of slope at higher intensities (above a few times 10^{13} W/cm^2) does not appear in our calculations. In fact we were unable to find reasonable values of the cross sections that would reproduce such an effect.

On the other hand, for the same photon energy there is very good agreement with the experiment for the ratio $\text{Ne}^{3+}/\text{Ne}^{2+}$ provided that the intensity of the second harmonic is not higher than 10^{-3} of the fundamental. We note here that the cross sections we obtain by scaling fit the experimental data well in this case, although our scaled value for $\sigma_{23}^{(2)}$ (1×10^{-50} $\text{cm}^4 \text{s}$) is different from the one suggested in Ref. [1] (4.5×10^{-51} $\text{cm}^4 \text{s}$). This could be attributed either to the fact that our approach, in which rate equations are explicitly solved, takes into account the time dependence of the various species production more accurately, or perhaps to pure coincidence since the cross sections we obtain by scaling do not represent an exact calculation.

IV. CONCLUSIONS

Our purpose in this paper was to obtain certain theoretical predictions pertaining to recent and ongoing experiments on multiple ionization of neon under soft-x-ray radiation of relatively high intensity and short pulse duration. At this initial stage of the field, no attempt at highly quantitative results was made. The theory was based on cross sections obtained mostly through scaling which could be viewed as the weakest aspect of the theory. Otherwise, the differential equations governing the evolution of the species during the pulse and the spatiotemporal dependence of the radiation employed in the calculations are well justified. The most reliable quantities for making contact with the experimental data should be the ratios of various ionic species as a function of radiation intensity and frequency, as they require no absolute calibra-

tion. Our findings are in reasonable accord with the reported data, given the present state of both theory and experiment. The expectation that, given the photon energies and intensities in the experiments, the outcome should be dominated by sequential stripping of electrons from the outer shell appears to be confirmed. Some discrepancies in detail between theory and experiment are not too surprising at this stage, providing at the same time focal points for further refinement of both. For theory, the next step should be the quantitative calculation of some few-photon ionization generalized cross sections, to serve as reference points for the more reliable extrapolation to higher-order processes, which can only be expected to be obtained through scaling. Nevertheless, even at this level of theory physical insight has been possible. For example, we have been able to pinpoint a rather sensitive dependence of the dominant pathway for the production of Ne^{2+} on the relative magnitude of the relevant cross sections. This suggests the need for a more detailed examination, both experimentally and theoretically, of the pathways involved. The possible role of resonance or near resonance with intermediate states needs to be examined further. It is safe to say that given the bandwidth of the source, one would not expect

major resonant enhancement of any of the ionic species and there has not been any clear evidence for that in the data available to us. Presumably future data may bring out such features, in which case a more detailed analysis employing a density matrix formulation might be in order. Finally, the temporal intensity fluctuations during the pulse might have played a role. Assuming, as it appears to be the case, that such fluctuations are indeed random, the source would probably correspond to a chaotic state of the field, in which case the yield of N -photon ionization is enhanced by a factor of N (Ref. [17]). Given, however, the low order of the processes involved in this work, this would mean an apparent enhancement of the relevant cross sections by factors of 2 or 6 which, in view of the semiquantitative character of the analysis and uncertainties in the magnitude of the intensity, would not make much difference at this point. Their effect can be easily included in a more quantitative study.

ACKNOWLEDGMENTS

Very useful discussions with L. A. A. Nikolopoulos, M. Richter, and U. Becker are gratefully acknowledged.

-
- [1] A. A. Sorokin, M. Wellhofer, S. V. Bobashev, K. Tiedtke, and M. Richter, *Phys. Rev. A* **75**, 051402(R) (2007).
 - [2] H. Wabnitz, A. R. B. de Castro, P. Gürtler, T. Laarmann, W. Laasch, J. Schulz, and T. Möller, *Phys. Rev. Lett.* **94**, 023001 (2005).
 - [3] H. Wabnitz *et al.*, *Nature (London)* **420**, 482 (2002).
 - [4] P. Lambropoulos and X. Tang, *J. Opt. Soc. Am. B* **4**, 821 (1987).
 - [5] D. Charalambidis, P. Lambropoulos, H. Schröder, O. Faucher, H. Xu, M. Wagner, and C. Fotakis, *Phys. Rev. A* **50**, R2822 (1994).
 - [6] M. Richter (private communication).
 - [7] P. Lambropoulos, L. A. A. Nikolopoulos, and M. G. Makris, *Phys. Rev. A* **72**, 013410 (2005); L. A. A. Nikolopoulos and P. Lambropoulos, *J. Phys. B* **39**, 883 (2006).
 - [8] A. Sorokin *et al.*, *Appl. Phys. Lett.* **89**, 221114 (2006).
 - [9] D. J. Kennedy and S. T. Manson, *Phys. Rev. A* **5**, 227 (1972).
 - [10] W. F. Chan, G. Cooper, X. Guo, and C. E. Brion, *Phys. Rev. A* **45**, 1420 (1992).
 - [11] R. J. Bartlett, P. J. Walsh, Z. X. He, Y. Chung, E.-M. Lee, and J. A. R. Samson, *Phys. Rev. A* **46**, 5574 (1992).
 - [12] J. M. Bizau and F. J. Wuilleumier, *J. Electron Spectrosc. Relat. Phenom.* **71**, 205 (1995).
 - [13] A. M. Covington *et al.*, *Phys. Rev. A* **66**, 062710 (2002).
 - [14] A. Saenz and P. Lambropoulos, *J. Phys. B* **32**, 5629 (1999).
 - [15] L. A. A. Nikolopoulos and P. Lambropoulos, *J. Phys. B* **34**, 545 (2001).
 - [16] L. A. A. Nikolopoulos and P. Lambropoulos, *J. Phys. B* **40**, 1347 (2007).
 - [17] P. Lambropoulos, *Adv. At. Mol. Phys.* **12**, 87 (1976).
 - [18] M. Venuti, P. Decleva, and A. Lisini, *J. Phys. B* **29**, 5315 (1996).
 - [19] J. Samson, Z. He, L. Yin, and G. Haddad, *J. Phys. B* **27**, 887 (1994).
 - [20] W. F. Chan, G. Cooper, and C. E. Brion, *Phys. Rev. A* **44**, 186 (1991).